Viscometry and Atomic Force Microscopy Studies of the Interactions of a Dimeric Cyanine Dye with DNA

Jason A. Bordelon, Karl J. Feierabend, Shabana A. Siddiqui, Laura L. Wright, and Jeffrey T. Petty*

Department of Chemistry, Furman University, Greenville, South Carolina 29613

Received: December 31, 2001; In Final Form: March 4, 2002

The structures of the noncovalent complexes of DNA with a thiazole orange dimer (TOTO) were investigated in solution and when adsorbed to a mica substrate, using viscometry and atomic force microscopy (AFM), respectively. From the viscosity measurements at low TOTO:base pair concentrations, the dye lengthens the DNA helix by two times the base pair spacing, consistent with bisintercalation. Higher concentrations of TOTO cause a significant decrease in the viscosity of the DNA solutions, as also observed for related bifunctional ligands. The conformational changes induced by the dimer are compared to those of the monomer. The contour lengths of the DNA-TOTO complexes adsorbed onto mica were directly measured by AFM. These lengths and the size of the binding site are inconsistent with the bisintercalation binding mode observed in solution, suggesting an alternative mode of binding on mica.

Introduction

Altering DNA recognition and expression are primary motivations for investigating the interaction of small molecules with DNA.[1] Besides directly inhibiting enzyme-DNA binding, small molecules can also induce DNA conformational changes, such as lengthening, bending, and stiffening, which may have biological relevance.[2] Noncovalent interactions of ligands with DNA include intercalation between the base pairs, major and minor groove binding, and electrostatic binding to the phosphates. The cyanine dyes are interesting because they exhibit all these modes of binding.[3−5] In addition, these dyes are utilized in the sensitive detection of single DNA molecules. For example, the positions of enzyme binding have been determined[6] and high-resolution DNA restriction maps have been constructed using the cyanine dyes.[7] Thus, it is relevant to understand how these noncovalently bound dyes alter the conformational properties of DNA.

In this work, the effects of the thiazole orange dimer TOTO (Figure 1) on the DNA conformation were investigated by two methods: solution viscometry and atomic force microscopy. When intercalators insert between the DNA base pairs, the resulting lengthening of the strands increases the viscosity of the solution.[8] Because groove binders do not cause helix lengthening, viscometry is an established method for determining the mode of ligand binding to DNA.[9] Short, rodlike DNA fragments are used to measure the extent of lengthening without the complication of helix stiffening and bending.[10] The elegant work of Reinert has shown that higher molecular weight DNA provides information about this bending and stiffening.[11] The goal of our studies is to determine if the DNA conformational changes induced by small molecules can be obtained more directly by atomic force microscopy (AFM). For example, helix lengthening,[12,13] bending,[14] compaction,[15] as well as changes in the tertiary structure,[16] have been investigated by AFM. Because single DNA molecules are analyzed, AFM offers the additional advantage of high sensitivity, which is significant when only small quantities of ligand are available or when ligand solubility limits viscometry studies. Finally, direct observation of DNA strands offers the capability of localizing binding sites on DNA strands.[17] A primary concern is how accurately the behavior of the immobilized DNA-small molecule complexes required for the AFM measurements approximates their behavior in solution. The negatively charged DNA strands are bound to atomically smooth mica using divalent metal cations (e.g. Mg^{2+} and Ni^{2+}). In previous studies with native DNA, a weak interaction between the DNA and the mica was postulated as the DNA strands rearrange on the surface, resulting in shapes that are characteristic of two-dimensional polymers.[18] As further support of the weak interaction, the immobilized DNA maintains a predominantly B-form at room temperature.[18,19] Also, the interaction of some planar, aromatic intercalators with DNA is not perturbed by the adsorption on mica.[12,13] For high concentrations of intercalator relative to DNA binding sites, the helix reaches a maximum extension as expected from an ideal lengthening of 0.34 nm/bound intercalator and from the number of available binding sites. In addition, the equilibrium constants measured

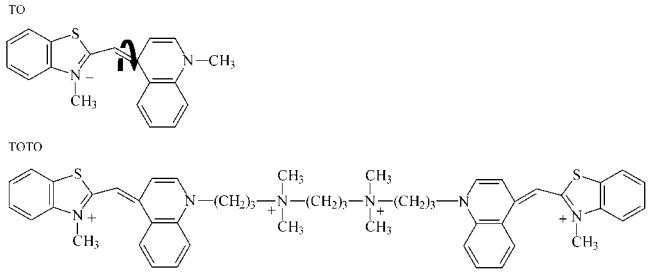

Figure 1. Chemical structures for the monomeric (TO) and the dimeric (TOTO) thiazole orange dyes used in these studies. The thiazole orange chromophore is nonplanar, and torsional twisting around the benzothiazole/quinoline bridge (see heavy arrow above) has a low energy barrier. The benzothiazole and quinoline adapt to the propeller twist of the base pairs by reducing the torsional angle from 47° when unbound to 22° when bound.[31,32]

* To whom correspondence should be addressed. Tel: (864) 294-2689; Fax: (864) 294-3559; e-mail: jeff.petty@furman.edu.

10.1021/jp014680j CCC: $22.00
Published on Web 04/17/2002

from the helix extension of the immobilized intercalator-DNA complexes agree with the measurements in solution.[12,13]

Below we describe structural studies of the DNA complexes with the thiazole orange dimer TOTO (Figure 1). Using solution viscosity measurements, the DNA structural changes caused by the bisintercalating dimer are compared with those caused by the monointercalating monomer TO (Figure 1). AFM was used to directly measure the contour lengths and binding site size of the immobilized TOTO/DNA complexes. The smaller lengths and the larger binding site are inconsistent with bisintercalation and suggest an alternative mode of binding. Reliable measurements of the extent of lengthening by TOTO could only be obtained when sufficient concentrations of Mg^{2+} or Na^+ were present. Gel electrophoresis experiments demonstrate that these cations assist in the equilibration of TOTO among the DNA binding sites.

Materials and Methods

Viscometry. Viscosity measurements were made with a Cannon-Ubbelohde semi-micro viscometer with a capillary diameter of 0.54 mm (Model 75, Cannon Instrument Company). The viscometer was submerged in a water bath to maintain a constant temperature of 27.00 ± 0.05 °C. All solutions were filtered through 0.2 μm filters (Pall Gelman, Acrodisc) prior to the measurements. The calf thymus DNA (Type I, 42% GC, Sigma) was sonicated to reduce its length using the following steps.[20] The DNA was first dissolved at a concentration of 2 mg/mL in a 1 M NaCl, 10 mM Tris/Tris-H^+ (Tris = tris-(hydroxymethyl)aminomethane) buffer with a pH of 7.5. The solution was purged with nitrogen during sonication and then dialyzed overnight against a 10 mM Tris/Tris-H^+, pH=7.5 buffer. Using the flow times between the viscometer timing marks of 107.6 ± 0.1 s for the buffer and 112.1 ± 0.1 s for a 0.304 mM DNA base pair (bp) solution, a viscosity average molecular weight was determined to be 3×10^5 g/mole bp[21] (confirmed by agarose gel electrophoresis), a size characteristic of rodlike DNA.[10] With no change in the axial width of these DNA strands, the lengthening by intercalating dyes is proportional to $[\eta]^{1/3}$, where $[\eta]$ is the intrinsic viscosity, the contribution to the solution viscosity due to the DNA.[22] Especially for the low DNA concentrations used in these experiments, the intrinsic viscosity is proportional to the difference in flow times for the buffer with and without DNA, resulting in the following equation:[23,24]

$$\frac{L}{L_o} = \frac{[\eta]^{1/3}}{[\eta]_o^{1/3}} = \frac{(t - t_b)^{1/3}}{(t_o - t_b)^{1/3}}$$

where L and L_o are the DNA lengths and $[\eta]$ and $[\eta]_o$ are the intrinsic viscosities in the presence and absence of dye, respectively. The flow times of the buffer, the DNA solution, and the DNA-dye solution are t_b, t_o, and t, respectively. The relative lengthening of the helix is obtained from the dependence of L/L_o on r, where r is the concentration of bound dyes/concentration of bp. The tosylate salt of the thiazole orange monomer (TO) was a gift of Becton Dickinson, and the iodide salt of the thiazole orange dimer (TOTO) was a gift of Molecular Probes. The dye solutions were stored at −20 °C and protected from room light. The concentrations of the dyes were determined using the molar absorptivities of 63,000 M^{-1} cm^{-1} for TO (500 nm, aqueous buffer) and 131,700 M^{-1} cm^{-1} for TOTO (507 nm, methanol).[4,25] Small aliquots of a concentrated dye solution (≈1 mM in 10 mM Tris/Tris-H^+) were added directly to the 1.03 mL DNA solution using a 10 μL syringe (Hamilton), modified with a glass tubing extension.[26] The dilution of the DNA solution was less than 5%, which was accounted for in the calculations. The cyanine dyes have limited solubility in aqueous solution, which was substantially increased by mild heating (55−60 °C). Precipitation at lower temperatures is slow, thus enabling quantitative transfer of the dye solution to the viscometer. The resulting solution was mixed by bubbling air through the viscometer and allowing equilibration for 2−3 min prior to the measurements. Given the low ionic strength of the buffer and the relatively high DNA concentration (0.3 mM), the high affinity of TO and TOTO for DNA results in negligible dissociation of the complex.[4,5] The flow times of the solutions between the timing marks were measured at least in triplicate. The error in the length measurements was propagated using standard procedures, and the uncertainties are reported as $\pm 1\sigma$.[27]

Atomic Force Microscopy. A Nanoscope IIIa (Digital Instruments) with the type E scanner, which has a maximum scan range of 12 μm × 12 μm, was used. The TESP tips (TappingMode Etched Silicon Probe, Digital Instruments) had an end-radius of curvature of ≈10 nm and a resonant frequency of 298−367 kHz. The tip was operated in tapping mode and was scanned at 5 lines/s. The images have a 512 × 512 pixel resolution over the 1 μm × 1 μm scan range. Images were collected only after the thermal drift in the piezo was negligible. Height variations in the background were removed by polynomial fitting (second order) of each scan line. The DNA strand lengths were determined using the tracing tools in NIH image (version 1.62) to determine the distance between user marked pixels on the DNA strand. This method has previously been demonstrated to be an accurate approach for measuring the DNA fragment lengths.[28] For example, our measured length of pUC19 DNA (2686 bp, 50.6% GC, Life Technologies) was 0.85 ± 0.04 μm (47 strands), or 5% smaller than the theoretical length expected for B-form DNA. This result compares favorably with previous measurements of native DNA immobilized on mica.[18] The dependence of contour lengths of the DNA-dye complexes on the number of bound dyes determines the absolute helix lengthening by the dyes.

For persistence length measurements, the procedure of Frontali et al. was used, which measures the average squared angle $\langle\theta^2\rangle$ between the vectors that define the DNA strand.[29] From the variation of $\langle\theta^2\rangle$ with the distance between the vectors (l), the persistence length (a) is determined: $\langle\theta^2\rangle = l/a$. The distance between the digitized points on the DNA strands was ≈2 nm, thus providing sufficient resolution to precisely measure the persistence length. This analysis was conducted using a locally written program for Igor Pro (version 4.04).

Supercoiled pUC19 DNA was linearized using the restriction endonuclease *Pst*I (Life Technologies). As in the viscosity studies, the DNA and TOTO were mixed in a higher salt buffer (10 mM Mg^{2+}, 10 mM Na^+, 10 mM Tris) to ensure equilibration. The solution contained 1 μM bp (3.7 nM pUC19 molecules) with varying concentrations of TOTO in the final volume of 20 μL. To be consistent with previous AFM studies, the DNA-TOTO complex was deposited on mica using a lower salt buffer. Thus, freshly cleaved mica was submerged in a large volume (1.5 mL) of a 2 mM Mg^{2+}, 10 mM Na^+, 1 mM Tris, and then the 20 μL of the previously equilibrated DNA-TOTO solution was pipetted on top of the mica. The resulting sample was incubated for thirty minutes and was washed by submerging in 3 mL of filtered (0.2 μm), deionized water for 1 min. Excess water was wicked away, and the sample was dried with nitrogen.

Gel Electrophoresis. For the gel electrophoresis studies, ϕX174 replicative form DNA (5386 bp, 44.7% GC, Life

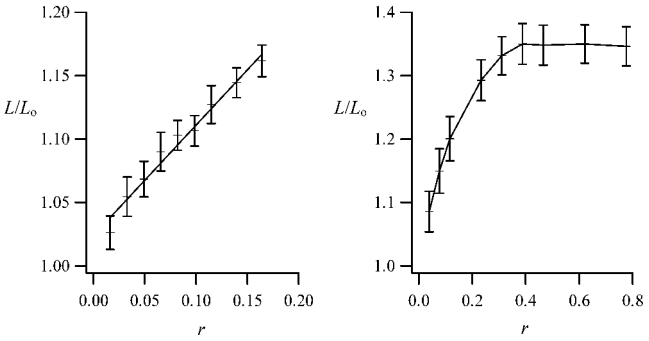

Figure 2. Graphs of the relative lengthening (L/L_o) of rodlike DNA fragments vs r (bound dyes/bp) for the thiazole orange monomer. At low binding ratios (left graph), a weighted least-squares fit results in an intercept of 1.01 ± 0.01 and a slope of 1.0 ± 0.1 base pairs/bound dye, a lengthening of the helix consistent with intercalation. At higher binding ratios (right graph), the sites saturate at about 0.4 bp/bound dye, corresponding to a site size of 2.5 bp/dye. A trend line is provided to emphasize the saturation of the binding sites. The error bars are $\pm 1\sigma$.

Technologies) was used. Following linearization by reaction with *Pst*I (Life Technologies), the DNA was purified using a silica-based, anion-exchange resin (Wizard DNA Cleanup Kit, Promega) to remove the Mg^{2+} needed for the restriction endonuclease cleavage. In a 0.5X TBE buffer (4.5 mM Tris, 4.5 mM boric acid, 0.1 mM EDTA), the DNA (0.25 μg), dye, and salt (Na^+, Mg^{2+}) solutions were combined. The resulting solution was loaded onto a 1% agarose gel in a 0.5X TBE buffer, and a voltage gradient of 9 V/cm was applied for 1−1.5 h. After electrophoresis, the gels were stained with ethidium bromide (1 μg/mL), and an image of the gel was obtained with an UV transilluminator (254 nm) and CCD camera (Ultra-Lum).

Results and Discussion

Viscometry−Thiazole Orange Monomer. Our preliminary solution viscometry measurements studied the structural changes in calf thymus DNA induced by the monomeric thiazole orange dye TO (Figure 1). Complex formation is strongly favored because of the high base pair concentrations (0.3 mM) and the relatively large association equilibrium constant (10^6 M^{-1}).[5] For example, for a stoichiometric ratio of 1 TO:10 bp ($r = 0.1$), 0.4% of the TO-DNA complexes are dissociated. From the change in the relative DNA length (L/L_o) with the amount of bound TO (r), each bound dye lengthens the helix by 1.0 ± 0.2 times the base pair spacing, with these values derived from three separate measurements (Figure 2). This lengthening is consistent with intercalation, and this mode of binding was also determined for a related monomeric oxazole yellow dye using flow linear and circular dichroism spectra.[30] Figure 2 shows that the DNA strand lengths do not change for concentrations higher than 0.4 dyes/bp, which suggests the number of available intercalation sites is limited to 2.5 bp/bound dye. As with AFM measurements, an additional estimate of the binding site size is obtained from the DNA extension when the intercalation sites are fully occupied.[12] The maximum relative lengthening, 1.35 times the base pair spacing for TO (Figure 2), depends on the number of available binding sites and on the extension induced by each bound dye (1.0 times base pair spacing). Thus, the 35% extension of the helix at saturation gives a site size of 3 bp. Both of these site size estimates agree with our previous measurements using the McGhee-von Hippel model to analyze the binding isotherms.[5] We obtained similar results for the association of the ethidium cation with DNA: a binding site size of 2−3 bp/dye and a helix lengthening of 0.9 ± 0.1 times the base pair spacing (from three separate measurements). This latter result agrees with previous experiments.[9] Previous spectroscopic, thermodynamic, and theoretical studies have suggested that thiazole orange interacts with DNA as an unfused intercalator (Figure 1).[5,31,32] The similarities with the fused ring intercalator ethidium suggests that thiazole orange does not bend the DNA helix, as do related nonplanar aromatic ligands.[33] This distinction is possibly due to the flexibility between the aromatic rings (Figure 1).[31,32]

Viscometry−Thiazole Orange Dimer. Having established the extent of lengthening and the mode of binding of the monomer, we used viscosity measurements to investigate how the dimer TOTO (Figure 1) associates with calf thymus DNA. Previous NMR spectra showed that bisintercalation is favored for certain base sequences, but broad spectral features indicated rapid exchange among other binding sites, thus opening the possibility for alternate modes of binding.[31] By comparison with the lengthening induced by the thiazole orange monomer (1.0 times the base pair spacing), a lengthening of only 1.3−1.5 times the base pair spacing was observed for the dimer. A possible explanation for this small lengthening is that the dimer interacts by a combination of bis and monointercalation,[34] as observed for a dimer of ethidium that is structurally similar to TOTO.[35] In addition, bisintercalation with helix bending[36,37] or intermolecular/intramolecular cross-linking of the DNA strands[38,39] could occur.

Another possibility is related to the dye distribution on the DNA. Because these +4 charged dyes alter the electrophoretic mobility of DNA strands, splitting of the DNA-TOTO bands (Figure 3, outer lanes) is most consistent with an inhomogeneous dye distribution, as opposed to other explanations such as intermolecular or intramolecular cross-linking.[40] The slow band is comprised of DNA fragments that bind most of the TOTO in solution with saturation of the intercalation sites at the 1 TOTO:4 bp ratio. As suggested by the width of the band, the remaining amount of TOTO is evenly distributed among the fragments in the fast band. The intensities of the two bands differ because of the efficiency of staining by ethidium. After the electrophoresis, the DNA was stained with ethidium because the fluorescence filter of the gel imaging system was optimized for this dye. The fragments that are saturated with TOTO will be less efficiently stained and hence will have a lower fluorescence intensity.[40] In addition, the fast band has more fragments and hence more binding sites for ethidium when the overall TOTO:bp stoichiometry is well below the saturation limit. For example, for a distribution of one TOTO to 4 bp (slow band) and 20 bp (fast band), an overall stoichiometry of 1 TOTO:10 bp results in three times more fragments in the fast band.

Carlsson et al. demonstrated that the equilibrium state, with a single DNA band and homogeneous dye distribution, is achieved by an increase in temperature.[40] Our gel electrophoresis studies using a 5386 bp fragment (ϕX174 DNA) show that equilibrium is also achieved at room temperature by increasing the ionic strength of the buffer. Figure 3 shows how the electrophoretic mobility of the ϕX174 DNA fragment, with a sub-saturating stoichiometry of 1 dye:10 bp, varies with the Mg^{2+} concentration. When the buffer contains no Mg^{2+}, the band splitting is evidence of the nonuniform dye distribution. With increasing amounts of Mg^{2+} in the buffer, the transition to a single band indicates that the dye becomes homogeneously distributed. The same result can be achieved with higher concentrations of Na^+ (Figure 3), which suggests that the ionic strength of the buffer determines the extent of equilibration.

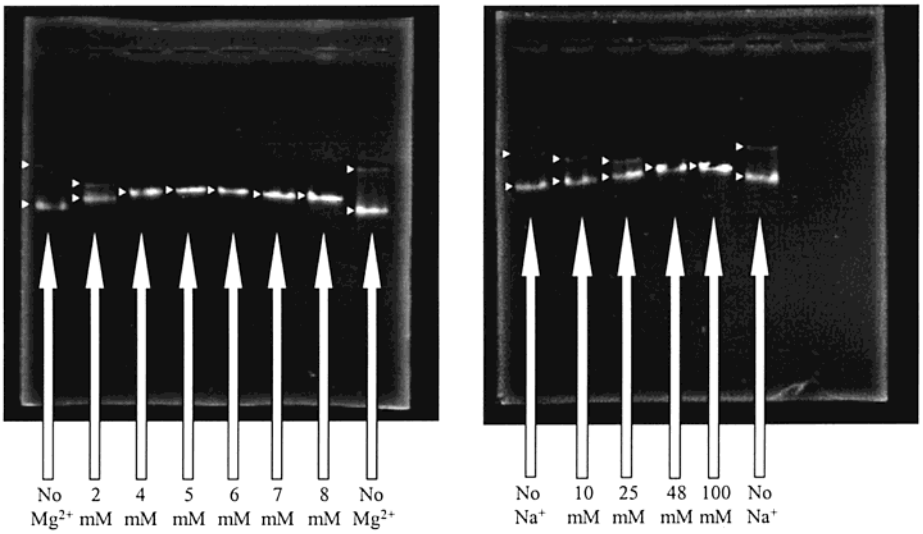

Figure 3. Electropherograms of ϕX174 DNA (0.25 mg) with a sub-saturating stoichiometry of 1 dye:10 bp in a 0.5X TBE buffer with varying amounts of Mg^{2+} (left) and Na^+ (right). The direction of the electric field is from negative (top) to positive (bottom). The white triangular marks are provided to more clearly identify the bands. The difference in the electrophoretic mobility is attributed to a large amount of bound TOTO for the fragments in the slow band and a small amount of bound TOTO in the fast band. With increasing cation concentrations, the mobilities of the fragments merge, which is consistent with a homogeneous dye distribution.

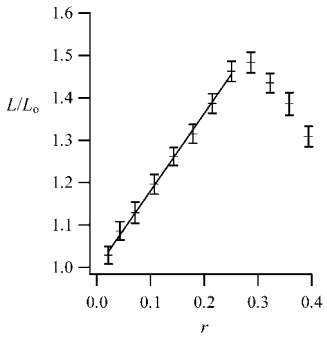

Figure 4. Graph of the relative lengthening (L/L_o) of rodlike DNA fragments vs r (bound dyes/bp) for the dimer TOTO. From a weighted least-squares fit, the lengthening is 2.0 ± 0.1 base pairs/bound dye, consistent with bisintercalation, and the intercept is 1.00 ± 0.02. The intrinsic viscosity decreases after 0.3 bound dye/bp, indicative of a significant conformational change in the DNA. The error bars are $\pm 1\sigma$.

TABLE 1: DNA-TOTO Contour Length Measurements

TOTO:bp[a]	length (μm)[b]	σ (μm)[c] − CV[d]
0	0.850	0.037 − 4.4%
1:50	0.878	0.033 − 3.7%
1:40	0.894	0.037 − 4.2%
1:30	0.906	0.038 − 4.2%
1:15	0.965	0.048 − 4.9%
1:10	1.003	0.044 − 4.3%
1:8	1.029	0.045 − 4.4%
1:6	1.033	0.054 − 5.5%
1:5	1.042	0.030 − 2.9%
1:4	1.069	0.056 − 5.3%
1:3	1.063	0.071 − 6.7%
1:2	1.131	0.049 − 4.4%
1:1	1.131	0.061 − 5.4%

[a] Concentration of TOTO:base pair (bp). [b] Contour lengths of the TOTO/DNA complexes in μm. [c] The standard deviations (σ) are $\pm 1\sigma$. [d] The coefficients of variation of the contour lengths (CV) are the standard deviation/contour length, expressed as a percent.

The cations may influence the extent of equilibration by competing with the dyes for DNA binding sites. As described by the counterion condensation theory, the high charge density of the DNA phosphates results in highly localized cation concentrations around the DNA.[41] Because the dimers bind so strongly to DNA,[4,5] the cations are not sufficiently concentrated to dissociate the DNA:dye complex, but competition for the binding sites could attenuate the interactions between the dimers.

Having established that sufficient concentrations of Mg^{2+} cause equilibration of the thiazole orange dimer with DNA, the viscosity studies with calf thymus DNA were repeated in a 10 mM Mg^{2+}, 10 mM Tris/Tris-H^+ buffer (Figure 4). At low dye:bp concentrations, we observed a lengthening of 2.0 ± 0.1 times the base pair spacing (from four separate measurements), which is twice that observed for the monomer and is thus consistent with bisintercalation. The linear increase in the relative lengthening (L/L_o) suggests this mode of binding continues to $r = 0.25-0.35$ dyes/bp. This transition, which occurs at a coverage of one TOTO for 3−4 bp, is consistent with the value of 4 bp/TOTO obtained from the 50% extension of the helix (using maximum extension of $L/L_o = 1.5$ in Figure 4) and with the 4 bp binding site measured in NMR studies.[31] The decrease in the solution viscosity at higher TOTO:bp concentrations, which was not observed for the monomer (Figure 2), is possibly due to intermolecular or intramolecular cross-linking of the DNA strands, as observed for other dimeric ligands.[36,38]

Atomic Force Microscopy−Thiazole Orange Dimer. We now describe AFM measurements to determine if the dye-DNA complexes immobilized on mica exhibit the lengthening observed in solution. TOTO has been used for these studies because it has a high affinity for DNA. Thus, dye-DNA complex dissociation is minimized in the dilute solutions needed to resolve individual DNA strands by AFM and in the washing steps needed to remove buffer salts from the mica surface. From our previous thermodynamic measurements of thiazole orange monomers, we estimate the association equilibrium constant to be 10^{14} M^{-1} for the interaction of the bisintercalating TOTO with the DNA binding site.[5] As an example, for a stoichiometry of 1 dye:4 bp, the percent of dissociated TOTO is 0.2% using a typical bp concentration of 13 nM. The contour lengths of pUC19 DNA when complexed with thirteen different TOTO:DNA bp ratios are summarized in Table 1. A total of 650 strands were analyzed. At each dye:bp concentration, the contour lengths of 40−60 strands were measured from three to five separately prepared samples. The resulting coefficients of variation (CV)

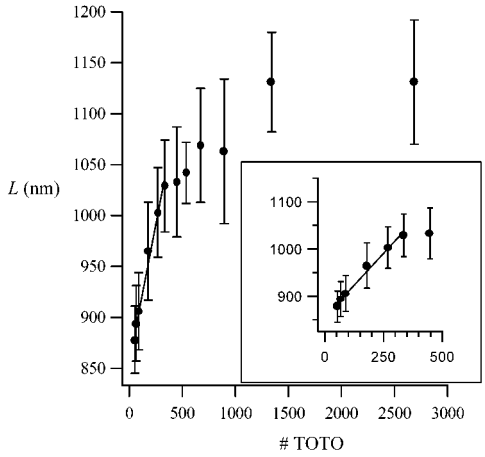

Figure 5. Graph of the contour lengths (L) of pUC19 DNA (2686 bp) vs the number of bound TOTO molecules. The inset shows the linear fit over the data from 1 TOTO:50 bp to 1 TOTO:8 bp. The slope measures the lengthening of the binding site by each TOTO to be 0.54 ± 0.16 nm. The intercept determines the length of the pUC19 in the absence of dye to be 0.86 ± 0.03 μm. This value agrees with our independent measurements of contour length of pUC19 to be 0.85 ± 0.04 μm. The error bars for the contour lengths are $\pm 1\sigma$.

for the contour lengths average 5%, which is reasonable based on previous studies of native DNA.[18,28] The structural changes in the DNA strands are assessed from Figure 5. At low dye concentrations (1 TOTO:50 bp to 1 TOTO:8 bp), the DNA contour lengths increase linearly with the number of bound dyes. The intercept predicts the length of the fragments in the absence of dye to be 0.86 ± 0.03 μm, in good agreement with our independent measurement of 0.85 ± 0.04 μm (Table 1). From the variation of the contour length with the number of bound dyes, each TOTO lengthens the helix by 0.54 ± 0.16 nm. Although the relative deviation of the contour lengths is small (CV $\approx$ 5%), the limited overall change in contour lengths contributes to a significant error for the slope in Figure 5. The range 0.54 ± 0.16 nm encompasses the helix extension observed in the solution viscosity measurements of two times the base pair spacing, or 0.68 nm. However, it is also possible that the mica causes TOTO to interact by a mixed mode of mono and bisintercalation, as 0.54 nm is 20% lower than the helix extension of TOTO in solution and is 60% higher than the helix extension of TO in solution. Below, we further consider this alternative mode of association.

At higher TOTO:bp concentrations, the contour lengths of the immobilized strands provide further insight into the mode of binding (Figure 5). Previous AFM studies of DNA complexes with the cationic monointercalators ethidium and daunomycin have shown that DNA strands lengthen as expected from the number of available binding sites and from an ideal extension of 0.34 nm/intercalator.[12,13] The binding site size, n, is calculated using $n = L_o/L_{sat-}L_o$, where L_o and L_{sat} are the contour lengths in the absence of ligand and when the binding sites are fully occupied by ligand, respectively. The site sizes for the above monointercalators agree with measurements in solution.[12] This equation shows that the interaction of TOTO with DNA differs for the adsorbed complexes and for the complexes in solution. First, the contour lengths of strands with subsaturating amounts of TOTO are less than observed in solution. In the viscometry measurements, the linearity of the relative lengthening suggests that bisintercalation occurs up to the site saturation of 1 TOTO:4 bp with a helix extension of 50% (Figure 4). For the adsorbed complexes, full occupancy of the binding sites should result in bisintercalation every four bases pairs, or intercalation every two base pairs ($n = 2$). Using $L_o = 0.85$ μm (Table 1), a contour length of 1.29 μm is calculated, while our measured length is 1.07 ± 0.06 μm. Besides the contour lengths, the binding site size also differs from that in solution. Using the contour lengths at the highest dye concentrations, $L_{sat} = 1.13$ μm, and $L_o = 0.85$ μm (Figure 5 and Table 1), each TOTO monointercalates every three base pairs. This result is clearly inconsistent with bisintercalation due to the length of the spermine linker between the thiazole orange chromophores.[4] One possible explanation for these smaller contour lengths and the larger binding site is that the dimer associates by a mixture of mono and bisintercalation. Favorable intermolecular interactions that have been suggested for other dimeric ligands could promote monointercalation of TOTO.[35,42] In addition, alternative modes of binding in the minor groove and to the exterior of DNA have been observed for cyanine dyes related to TOTO.[3,30] While intermolecular associations should be more prevalent when the number of dyes exceed the available intercalation sites,[30] the contour lengths are significantly shorter that expected even for subsaturating concentrations (<1 TOTO:4 bp). This latter observation suggests that the change in binding mode of the adsorbed complexes is due to the mica, which is reasonable given that the mica and the dyes are oppositely charged. In support of favorable interactions between the dyes and mica, some cyanine dyes aggregate on mica.[43] To further investigate whether the dimer binds by a mixed mode, we will measure the helix lengthening and the binding site size of the monomer using a fluid cell attachment for the AFM. Because of the much weaker monomer-DNA affinity and of the low DNA concentrations in the AFM solutions, larger concentrations of dye are needed for measurable lengthening. While these high concentrations have caused significant residue buildup in our dry samples, the aqueous environment will eliminate this complication.

The smaller than expected lengths of the adsorbed DNA-TOTO complexes may also be related to dehydration. This hypothesis has been proposed from contour length measurements of native DNA both at low and room temperatures,[19,44] and we will investigate this issue by using the fluid cell to maintain the aqueous environment of the strands. Finally, it is also possible that the nonplanar orientation of the benzothiazole and quinoline rings influences the structure of the complex (Figure 1).[31] Smaller than expected changes in the solution viscosity of related nonplanar unfused intercalators have been attributed to helix bending.[33] Our persistence length measurements of the TOTO-DNA complexes do not reflect such changes. For example, for native DNA, we measured a persistence length of 50 ± 20 nm, which is consistent with previous measurements of DNA strands both in solution and immobilized on mica.[18,45] Even up to 1 TOTO:1 bp, we observe no difference between persistence lengths at the various TOTO:bp concentrations. The uncertainties (15−25 nm) may obscure variations in the persistence lengths, a limitation that has been observed in previous microscopy based measurements.[29,46] We are now exploring the role of the dye structure by examining the DNA lengthening using a related oxazole yellow dimer because its aromatic rings are coplanar.[32]

Conclusions

Atomic force microscopy is an important tool for the study of small molecule-DNA interactions because structural changes are directly measured. The goal of our studies is to compare how the thiazole orange dye TOTO influences the conformation of DNA in solution, as measured by viscometry, and immobilized on mica, as measured by AFM. At low dye:bp

concentrations in solution, the bisintercalating TOTO lengthens the DNA helix by 2.0 ± 0.1 times the base pair spacing. At higher dye:bp concentrations, the mode of binding of TOTO with DNA changes, as reflected by a significant decrease in the solution viscosity. The monomeric TO causes a lengthening of one-half that observed for the dimer (1.0 ± 0.2 times the base pair spacing), but it does not decrease the solution viscosity at higher dye concentrations. For the TOTO-DNA complexes adsorbed onto mica, the lengthening of 0.54 ± 0.16 nm/TOTO, or 1.6 ± 0.5 times the base pair spacing, suggests a mixed mode of mono and bisintercalation. Also suggesting that TOTO associates by a mode other than bisintercalation are the contour lengths and binding site sizes with higher amounts of bound dye. Possible sources of this difference between the behavior in solution and on the mica surface are favorable intermolecular interactions between the bound dyes and the mica, dehydration of the samples, and nonplanar structure of the thiazole orange chromophore. No significant variation in the persistence lengths of the complexes was observed over the range of dye concentrations, suggesting that the dye is not causing significant helix bending. Finally, the dimeric dyes bind inhomogeneously to the DNA helix, a pertinent issue for single DNA fragment measurements based on the fluorescence intensity.[47] We have shown that equilibration is achieved when the cation concentrations are greater than 4 mM Mg^{2+} or 48 mM Na^{+}.

Acknowledgment. We thank D. Wilson for helpful comments. We gratefully acknowledge T. Ward and C.-H. Chen of Becton Dickinson for the gift of thiazole orange. We also gratefully acknowledge V. Singer of Molecular Probes for the gift of TOTO. The financial support of Research Corporation, the National Institutes of Health, the National Science Foundation, the Independent Colleges and Universities of South Carolina, the Furman University Research and Professional Growth Fund, and the Furman Advantage Research Fellowship Program is greatly appreciated.

References and Notes

(1) (a) Wemmer, D. E. *Annu. Rev. Biophys. Biomol. Struct.* **2000**, *29*, 439. (b) Ren, J.; Chaires, J. B. *Methods Enzymol.* **2001**, *340*, 99.
(2) Reinert, K.-E. *J. Biomol. Struct. Dyn.* **1999**, *17*, 311.
(3) (a) Seifert, J. L.; Connor, R. E.; Kushon, S. A.; Wang, M.; Armitage, B. A. *J. Am. Chem. Soc.* **1999**, *121*, 2987. (b) Wang, M.; Silva, G. L.; Armitage, B. L. *J. Am. Chem. Soc.* **2000**, *122*, 9977. (c) Mikheikin, A. L.; Zhuze, A. L.; Zasedatelev, A. S. *J. Biomol. Struct. Dyn.* **2000**, *18*, 59.
(4) Rye, H. S.; Yue, S.; Wemmer, D. E.; Quesada, M. A.; Haugland, R. P.; Mathies, R. A.; Glazer, A. N. *Nucleic Acids Res.* **1992**, *20*, 2803.
(5) Petty, J. T.; Bordelon, J. A.; Robertson, M. E. *J. Phys. Chem. B* **2000**, *104*, 7221.
(6) Taylor, J. R.; Fang, M. M.; Nie, S. *Anal. Chem.* **2000**, *72*, 1979.
(7) Meng, X.; Cai, W.; Schwartz, D. C. *J. Biomol. Struct. Dyn.* **1996**, *13*, 945.
(8) Lerman, L. S. *J. Mol. Biol.* **1961**, *3*, 18.
(9) Suh, D.; Chaires, J. B. *Bioorg. Med. Chem.* **1995**, *3*, 723.
(10) Cohen, G.; Eisenberg, H. *Biopolymers* **1966**, *4*, 429.
(11) Reinert, K.-E.; Zimmer, Ch.; Arcamone, F. *J. Biomol. Struct. Dyn.* **1996**, *14*, 245.
(12) (a) Coury, J. E.; McFail-Isom, L.; Williams, L. D.; Bottomley, L. A. *Proc. Natl. Acad. Sci.* **1996**, *93*, 12283. (b) Coury, J. E.; Anderson, J. R.; McFail-Isom, L.; Williams, L. D.; Bottomley, L. A. *J. Am. Chem. Soc.* **1997**, *119*, 3792.
(13) Lillehei, P. T.; Bottomley, L. A. *Methods Enzymol.* **2001**, *340*, 234.
(14) Hansma, H. G.; Browne, K. A.; Bezanilla, M.; Bruice, T. C. *Biochemistry* **1994**, *33*, 8436.
(15) (a) Pietrasanta, L. I.; Smith, B. L.; MacLeod, M. C. *Chem. Res. Toxicol.* **2000**, *13*, 351. (b) Onoa, G. B.; Cervantes, G.; Moreno, V.; Prieto, M. J. *Nucleic Acids Res.* **1998**, *26*, 1473.
(16) (a) Pope, L. H.; Davies, M. C.; Laughton, C. A.; Roberts, C. J.; Tendler, S. J. B.; Williams, P. M. *J. Microsc.* **2000**, *199*, 68. (b) Utsuno, K.; Tsuboi, M.; Katsumata, S.; Iwamoto, T. *Chem. Pharm. Bull. (Toyko)* **2001**, *49*, 413.
(17) (a) Sun, H. B.; Yokata, H. *Anal. Chem.* **2000**, *72*, 3138. (b) Seong, G. H.; Niimi, T.; Yanagida, Y.; Kobatake, E.; Aizawa, M. *Anal. Chem.* **2000**, *72*, 1288.
(18) Rivetti, C.; Guthold, M.; Bustamante, C. *J. Mol. Biol.* **1996**, *264*, 919.
(19) Rivetti, C.; Codeluppi, S. *Ultramicroscopy* **2001**, *87*, 55.
(20) Pyeritz, R. E.; Schlegel, R. A.; Thomas, C. A., Jr. *Biochim. Biophys. Acta* **1972**, *272*, 504.
(21) Doty, P.; McGill, B. B.; Rice, S. A. *Proc. Natl. Acad. Sci. U.S.A.* **1958**, *44*, 432.
(22) Cohen, G.; Eisenberg, H. *Biopolymers* **1969**, *8*, 45.
(23) Wakelin, L. P. G.; Waring, M. J. *Biochem. J.* **1976**, *157*, 721.
(24) Cantor, C. R.; Schimmel, P. R. *Biophysical Chemistry*; W. H. Freeman: New York, 1980.
(25) Nygren, J.; Svanvik, N.; Kubista, M. *Biopolymers* **1998**, *46*, 39.
(26) Davidson, M. W.; Griggs, B. G.; Boykin, D. W.; Wilson, W. D. *J. Med. Chem.* **1977**, *20*, 1117.
(27) Bevington, P. R.; Robinson, D. K. *Data Reduction and Error Analysis for the Physical Sciences;* McGraw-Hill: New York, 1992.
(28) Fang, Y.; Spisz, T. S.; Wiltshire, T.; D'Costa, N. P.; Bankman, I. N.; Reeves, R. H.; Hoh, J. H. *Anal. Chem.* **1998**, *70*, 2123.
(29) Frontali, C.; Dore, E.; Ferrauto, A.; Gratton, E.; Bettini, A.; Pozzan, M. R. *Biopolymers* **1979**, *18*, 1353.
(30) Larsson, A.; Carlsson, C.; Jonsson, M.; Albinsson, B. *J. Am. Chem. Soc.* **1994**, *116*, 8459.
(31) (a) Jacobsen, J. P.; Pedersen, J. B.; Hansen, L. F.; Wemmer, D. E. *Nucleic Acids Res.* **1995**, *23*, 753. (b) Spielmann, H. P.; Wemmer, D. E.; Jacobsen, J. P. *Biochemistry* **1995**, *34*, 8542.
(32) Johansen, F.; Jacobsen, J. P. *J. Biomol. Struct. Dyn.* **1998**, *16*, 205.
(33) Wilson, W. D.; Stekowski, L.; Tanious, F. A.; Watson, R. A.; Mokrosz, J. L.; Stekowska, A.; Webster, G. D.; Neidle, S. *J. Am. Chem. Soc.* **1988**, *110*, 8292.
(34) (a) Wakelin, L. P. G.; Romanos, M.; Chen, T. K.; Glaubiger, D.; Canellakis, E. S.; Waring, M. J. *Biochemistry* **1978**, *17*, 5057. (b) McFadyen, W. D.; Sotirellis, N.; Denny, W. A.; Wakelin, L. P. G. *Biochim. Biophys. Acta* **1990**, *1048*, 50. (c) Denny, W. A.; Atwell, G. J.; Willmott, G. A.; Wakelin, L. P. G. *Biophys. Chem.* **1985**, *22*, 17.
(35) Gaugain, B.; Barbet, J.; Capelle, N.; Roques, B. P.; Le Pecq, J.-B. *Biochemistry* **1978**, *17*, 5078.
(36) Müller, W.; Crothers, D. M. *J. Mol. Biol.* **1968**, *35*, 251.
(37) Peek, M. E.; Lipscomb, L. A.; Bertrand, J. A.; Gao, Q.; Roques, B. P.; Garbay-Jaureguiberry, C.; Williams, L. D. *Biochemistry* **1994**, *33*, 3794.
(38) Le Pecq, J.-B.; Le Bret, M.; Barbet, J.; Roques, B. *Proc. Natl. Acad. Sci. U.S.A.* **1975**, *72*, 2915.
(39) Huang, C.-H.; Mirabelli, C. K.; Mong, S.; Crooke, S. T. *Cancer Res.* **1983**, *43*, 2718.
(40) Carlsson, C.; Jonsson, M.; Åkerman, B. *Nucleic Acids Res.* **1995**, *23*, 2413.
(41) Manning, G. S.; Ray, J. *J. Biomol. Struct. Dyn.* **1998**, *16*, 461.
(42) Leng, F.; Priebe, W.; Chaires, J. B. *Biochemistry* **1998**, *37*, 1743.
(43) Yao, H.; Sugiyama, S.; Kawabata, R.; Ikeda, H.; Matsuoka, O.; Yamamoto, S.; Kitamura, N. *J. Phys. Chem. B* **1999**, *103*, 4452.
(44) Feng, X. Z.; Bash, R.; Balagurumoorthy, P.; Lohr, D.; Harrington, R. E.; Lindsay, S. M. *Nucleic Acis Res.* **2000**, *28*, 593.
(45) Hagerman, P. J. *Annu. Rev. Biophys. Chem.* **1988**, *17*, 265.
(46) (a) Hansma, H. G.; Kim, K. J.; Laney, D. E.; Garcia, R. A.; Argaman, M.; Allen, M. J.; Parsons, S. M. *J. Struct. Biol.* **1997**, *119*, 99. (b) Schulz, A.; Mücke, N.; Langowski, J.; Rippe, K. *J. Mol. Biol.* **1998**, *283*, 821.
(47) (a) Goodwin, P. M.; Johnson, M. E.; Martin, J. C.; Ambrose, W. P.; Marrone, B. L.; Jett, J. H.; Keller, R. A. *Nucleic Acids Res.* **1993**, *21*, 803. (b) Huang, Z.; Petty, J. T.; O'Quinn, B. L.; Longmire, J. L.; Brown, N. C.; Jett, J. H.; Keller R. A. *Nucleic Acids Res.* **1996**, *24*, 4202. (c) Van Orden, A.; Keller, R. A.; Ambrose, W. P. *Anal. Chem.* **2000**, *72*, 37.